Solvent Kinetic Isotope Effects Monitor Changes in Hydrogen Bonding at the Active Center of Yeast Pyruvate Decarboxylase Concomitant with Substrate Activation: The Substituent at Position 221 Can Control the State of Activation[†,‡]

Wen Wei, Min Liu, and Frank Jordan*

Department of Chemistry and Program in Cellular and Molecular Biodynamics, Rutgers, the State University of New Jersey, Newark, New Jersey 07102 USA

Received June 20, 2001; Revised Manuscript Received September 18, 2001

ABSTRACT: Substrate activation of yeast pyruvate decarboxylase has been studied extensively in the authors' laboratories providing strong evidence that interaction of substrate with residue C221 provides the trigger, and the information is then transmitted along the C221 to H92 to E91 to W412 to G413 pathway to the 4′-amino nitrogen of the thiamin diphosphate cofactor. Earlier, it was found that the C221S substitution reduced the Hill coefficient from 2.0 to 0.8−0.9, the C221A substitution to 1.0, even though C221 is located on the β domain some 20 Å from the active center thiamin diphosphate cofactor, which is at the interface of the α and γ domains. Here are reported experiments on the C221D/C222A and C221E/C222A variants, in which a negative charge is built onto the C221 side chain, to better mimic the effect of a pyruvate molecule covalently bonded to C221 as a thiohemiketal. Both variants were purified to an optimal activity of 70% of the wild-type enzyme, higher activity than that with the earlier uncharged substitutions at this position. The Hill coefficient for both variants is exactly 1.0. The deuterium solvent kinetic isotope effects (SKIE) on k_{cat} for these variants were similar to that for the wild-type enzyme and the C221A/C222A variant, suggesting that starting with the first irreversible step (decarboxylation) the rate-limiting transition states are very similar for all of these enzyme forms. In contrast, such SKIE on k_{cat}/K_m are quite different for the C221A/C222A variant (0.62) than for the C221E/C222A or C221D/C222A variants (0.80−0.82), clearly indicating the effect of the C221 substitutions on transition states starting with the binding of the first substrate to the enzyme and terminating with the decarboxylation step. The results provide strong additional evidence for the involvement of residue C221 in the substrate activation process and suggest that the C221D (C221E) substitution shifts the enzyme into a conformation that resembles the activated conformation. A comparison with SKIE for the wild-type enzyme provides insight to changes in hydrogen bonding at the active center as a result of substrate activation.

The thiamin diphosphate (ThDP)[1]-dependent enzyme pyruvate decarboxylase (E.C. 4.1.1.1) isolated from most sources except *Zymomonas mobilis* appears to display sigmoidal steady-state v_o-[S] plots, i.e., it is subject to homotropic activation. The substrate activation can also be deduced from pre-steady-state kinetic measurements, if the alcohol dehydrogenase/NADH coupled assay is used to monitor the rate of formation of the acetaldehyde via its subsequent reduction to ethanol, by monitoring the time-dependent depletion of NADH on the millisecond to second time-scale. In a series of studies from the authors' laboratories (*1*−*8*), the case has been made for the substrate activation pathway on yeast pyruvate decarboxylase (YPDC) being triggered by covalent or noncovalent interaction of pyruvate with residue C221. The initial impetus to undertake systematic studies of the cysteines as potential sites for substrate activation was the discovery that cysteine-specific reagents altered the Hill coefficient of the enzyme (*9*).

The X-ray structures of YPDCs from two yeast strains (*10*, *11*) confirmed the existence of only four cysteines, at positions 69, 152, 221, and 222, with C221 on the β domain being the nearest to the active center, some 20 Å from ThDP located at the interface of the α and γ domains. Systematic studies demonstrated the following: (i) Substitution of C221, but not of C222 (or the remaining two cysteines), abolished cooperativity (*1*, *2*) and indicated that likely C221 is

† This work was supported at Rutgers by NIH GM-50380, the NSF Training Grant-BIR 94/13198 in Cellular and Molecular Biodynamics (F.J., PI), the Rutgers University Busch Biomedical Fund, and Roche Diagnostics Corporation, Indianapolis, IN.

‡ The senior author wishes to dedicate this paper (belatedly) to his Ph.D. mentor Prof. Edward Thornton at the University of Pennsylvania, a pioneer in kinetic isotope effect studies, on the occasion of his 65th birthday.

* To whom correspondence should be addressed: Tel. 973-353-5470, FAX: 973-353-1264, E-mail: frjordan@newark.rutgers.edu.

[1] Abbreviations: ThDP, thiamin diphosphate; *scpdc1*, wild-type pyruvate decarboxylase gene isolated from *Saccharomyces cerevisiae*; YPDC, yeast pyruvate decarboxylase (EC.4.1.1.1) from *Saccharomyces cerevisiae* overexpressed in *Escherichia coli*; C221A/C222A, C221S/C222S, C221S, C221D/C222A, and C221E/C222A are variants created by mutations on the *scpdc1*; SKIE, deuterium solvent kinetic isotope effects; $^{D}k_{cat}$, k_{cat} at the pH plateau measured in water divided by k_{cat} at the pD plateau measured in deuterium oxide; $^{D}k_{cat}/K_m$, k_{cat}/K_m at the pH optimum measured in water divided by k_{cat}/K_m at the pD optimum measured in deuterium oxide; n_H, the Hill coefficient; ZmPDC, pyruvate decarboxylase isolated from *Zymomonas mobilis*; BFD, benzoylformate decarboxylase.

10.1021/bi0112964 CCC: $22.00
Published on Web 12/14/2001

dissociated, while H92, across the domain divide on the α domain, is protonated near the pH optimum of the enzyme (*3*). (ii) The information from pyruvate bound at C221 is transmitted to H92 (*4*). (iii) The residue C221 was shown to form a covalent product with the cinnamaldehyde produced from a mechanism-based inhibitor/alternate substrate, likely via a Michael addition, signaling the high reactivity of C221 (*5*), and providing the only protein chemical evidence for possible reaction at C221 so far. (iv) It was shown that substitution at E91 (*6*) and W412 (*7*) also would lead to abolition of substrate activation. The curious behavior of the C221S and C221S/C222S variants with Hill coefficients < 1.0 prompted further mutagenesis work and led to creation of the C221A, C222A, and C221A/C222A variants, of which those with the C221A substitution gave a Hill coefficient of 1.0 within experimental error (*4*). Parenthetically, the doubly substituted variants with the C222A substitution are used for the present work as well, to make certain that there would be no ambiguity introduced by any interactions with the C222 residue. Importantly, all of the C221 variants are active enzyme forms, even though they show no activation, counter to the notion that enzyme with no activation is inactive, advocated with the earlier accepted kinetic model for YPDC (*12*).

In an earlier paper, we found that reaction of the C222S/H92C variant with 1,3-dibromoacetone gave an enzyme species that appeared to be converted to an activated form of the enzyme (*4*). Also, recently we used the C221A/C222A variant to gather more support for our working hypothesis, that information from C221 is transmitted to the active center (*8*). Most notably, the rate of C2H/D exchange of ThDP, as an indicator of the rate of the first obligatory step in catalysis, was shown to be slower for the C221A/C222A variant than for the wild-type YPDC. The deuterium solvent kinetic isotope effects (SKIE) were determined for the same variant, providing a normal value for $^{D}k_{cat}$ (ca. 1.30), but a strongly inverse one for $^{D}k_{cat}/K_m$ (0.62). This experiment in essence ruled out the possibility that C221 was responsible for the inverse SKIE reported for the wild-type YPDC, and also suggested that the $^{D}k_{cat}$ SKIEs are quite similar for all species of pyruvate decarboxylase, both YPDC and from *Zymomonas mobilis* (ZmPDC; *13*) and indeed for the related enzyme benzoylformate decarboxylase (BFD; *14*).

Equipped with this information, we here report results of a study of the C221D/C222A and C221E/C222A variants, with the expectation that the lengthened side chain may bring the negative charge sufficiently proximal to the H92 imidazolium ring to afford a good mimic of the putative, covalent thiohemiketal adduct formed between C221 and pyruvate. We here summarize preparation of, steady-state kinetics with, and SKIEs on the C221D/C222A and C221E/C22A variants. The variants are nearly as active as the wild-type enzyme, yet show no substrate activation in the steady-state kinetics. Perhaps most significantly, the $^{D}k_{cat}/K_m$ SKIEs are less inverse on these variants than on the C221A/C222A variant, a somewhat less active variant. Such SKIE studies were also carried out on the wild-type enzyme over a broad pH/pD range, so that the results could be reliably compared with those on the variants. While our results are in accord with those reported for the $^{D}k_{cat}/K_m$ and $^{D}k_{cat}$, i.e., at very low and at saturating substrate concentrations (*12*), our values at the intermediate substrate concentration range, that pertain to transition states starting with substrate-activated enzyme and culminating in decarboxylation, are not inverse.

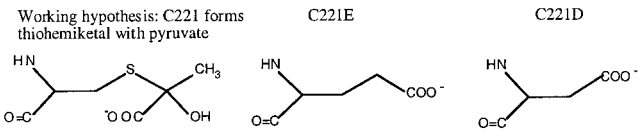

The SKIE results are found to be effective in signaling subtle changes in the structure. The results are consistent with the proposed role for C221, even though the substrate surrogate pyruvamide was not found at this position in the X-ray structure of YPDC in the presence of 300 mM pyruvamide (*15*). Experiments were presented elsewhere to show that pyruvamide and pyruvate are different enough as to make such comparisons ambiguous (*16*). Indeed, it is also shown here that addition of pyruvamide signals inhibition, rather than activation of the C221D/C222A and C221E/C22A variants. The SKIE results at *all* substrate concentrations are pertinent to hydrogen bonding changes at the active center, rather than originating from C221, and provide insight to changes in fractionation factors resulting from substrate activation.

EXPERIMENTAL PROCEDURES

Materials. The Quick-change site-directed mutagenesis kit was purchased from Stratagene. BL21(DE3) competent cells were purchased from Novagene. Dye Terminator Cycle Sequencing Ready Reaction kit was obtained from Applied Biosystems. The Wizard plasmid miniprep kit was obtained from Promega. Pyruvic acid sodium salt, alcohol dehydrogenase (ADH), and β-NADH were from Sigma. Talon metal affinity resin was from Clontech Laboratories, Inc. All of the primers were synthesized by Integrated DNA Technologies. 99.9% D_2O was purchased from Isotech. Other materials, including the chemicals to prepare the buffers, were all of the highest purity commercially available.

Construction of C221D/C222A and C221E/C222A Variants. Mutagenesis to produce the C221D/C222A and C221E/C222A variants was performed with the QuickChange site-directed mutagenesis kit following the manufacturers' instructions. In the PCR reaction, the pET22b (+) vector with the gene corresponding to the YPDC C222A variant was denatured and annealed with two mutagenic primers. These primers were 5′-GTT ATC TTG GCT GAT GCT **GAT** GCT TCC AGA CAC GAC GTC-3′ and 5′-GAC GTC GTG TCT GGA AGC **ATC** AGC ATC AGC CAA GAT AAC-3′ for C221D/C222A and 5′-GTT ATC TTG GCT GAT GCT **GAA** GCT TCC AGA CAC GAC GTC-3′ and 5′-GAC GTC GTG TCT GGA AGC **TTC** AGC ATC AGC CAA GAT AAC-3′ for C221E/C222A

The cysteine at the position 221 was changed to aspartic acid in the C221D/C222A variant, and to glutamic acid in the C222E/C222A variant by changing the nucleotide sequence at position 221 from TGT to GAT and GAA, respectively. The resulting PCR product was digested with *Dpn*I restriction enzyme and transformed to *Escherichia coli* XL 1-Blue competent cells. The cells were grown on LB-ampicillin agar plates overnight.

DNA Sequencing. The desired mutations were confirmed by DNA sequencing. Single colonies were picked from the plates and grown in 10 mL of LB-ampicillin at 37 °C with shaking at 300 rpm for 14 h. Plasmids were purified with the Wizard Plasmid Miniprep kit from Promega according to manufacturers' instructions. The purity of the plasmid was checked on a 0.8% agarose gel, and the concentration was determined by comparing to Lambda *Eco*I + *Hind*III markers (from Promega). Sequencing of the plasmids was carried out with the Dye Terminator Cycle Sequencing Ready Reaction kit from Applied Biosystems on an ABI 373 sequencer. *The entire gene*s of both mutants were sequenced using the primers listed below, and no mutations other than those desired were detected.

T7P	5′-CCGCGAAATTAATACGACTCACTATA-3′
T7T	5′-GTTATGCTAGTTATTGCTCAGCGGT-3′
AA67	5′-TGTCTTGTATCATCACCACCTTCG-3′
AA179	5′-AAGTTGTTGCAAACTCCAATGAC-3′
AA276	5′-CCGTTGAATCTGCTGACTTGATT-3′
AA376	5′-ACTTCTTGCAAGAAGGTGATGTTG-3′
AA483	5′-CCAAAGGCTCAATACAACGAAAT-3′

Enzyme Expression and Purification. The BL21(DE3) competent cells were transformed with plasmids containing the DNA precursors of the C221D/C222A and C221E/C222A variants for protein overexpression.

The BL21(DE3) cells with the mutated plasmids were grown in LB medium (10 g of tryptone, 5 g of yeast extract, 10 g of NaCl, and 50 mg of ampicillin/L) at 37 °C with shaking at 300 rpm to a A_{600} of 1.0−1.2. Overexpression of the YPDC genes was induced by adding 0.5 mM IPTG, 0.5 mM thiamin chloride, and 1 mM $MgCl_2$, and the cells were grown for an additional 3−4 h with shaking at 37 °C.

The wild-type YPDC with a His_6 tag attached to its C-terminus (*8*, *18*) was purified on a Talon metal affinity resin. The cells were harvested and washed with 20 mM potassium phosphate buffer (pH 6.8), containing 0.5 mM EDTA-2Na. The washed cells were resuspended in sonication buffer containing 50 mM NaPi, 100 mM NaCl, 2 mM $MgCl_2$, and 1 mM ThDP. The cell suspension was disrupted at 20 kHz in an ice−water bath for 4 min (10 s on, 10 s off) on a model 500 Sonic dismembrator (Fisher Scientific), then centrifuged at 23 203 rcf at 4 °C for 30 min. The supernatant was applied to Talon metal affinity resin equilibrated with sonication buffer. The column with the YPDC protein complexed to it was washed with sonication and washing buffer (50 mM MES, 100 mM NaCl, 2 mM $MgCl_2$, and 1 mM ThDP) stepwise, then eluted by eluting buffer (200 mM imidazole, 50 mM NaPi, 2 mM $MgCl_2$, and 1 mM ThDP). Fractions (2 mL) were collected and checked for protein content and YPDC activity. SDS−PAGE was used to check the purity of the fractions. The combined fractions were dialyzed against dialysis buffer (pH 6.0, 20 mM MES, 20 mM NaPi, 5 mM $MgCl_2$, 1 mM ThDP, and 0.1 mM EDTA) at 4 °C overnight and concentrated to less than 1 mL by using an Amicon Centriprep-30 device. Glycerol was added to the preparation to a final concentration of 30−50% for long-term storage. It was shown elsewhere that YPDC carrying the C-terminal His_6 tag is identical in every respect to the wild-type enzyme without the tag (*18*).

The C221D/C222A and C221E/C222A variants did not carry the C-terminal His_6 tag. These variants were purified on a Pharmacia Hiload Q Sep (HP) column using a Pharmacia FPLC system with the FPLC Director computer program. Steps of harvesting, cell washing, and sonication were exactly the same as with the WT YPDC purification, except the sonication buffer consisted of 20 mM KPi, 1 mM EDTA, 2 mM $MgCl_2$, 1 mM ThDP, and 1 mM PMSF. After sonication, the cells were centrifuged at 23 203 rcf for 30 min. The precipitate was discarded and ammonium sulfate was added to the supernatant to a final concentration of 1.5 M. The solution was stirred on an ice−water bath for 15−20 min, and then centrifuged at 23 203 rcf for 20 min. Ammonium sulfate was added to the supernatant to a final concentration of 2.8 M, and the solution was stirred for 15−20 min in an ice−water bath. The solution was centrifuged at 23 203 rcf for another 20 min. The pellet containing crude enzyme was dissolved in 20 mM Bis-Tris (pH 6.80), 0.5 M EDTA, 2 mM $MgCl_2$, 1 mM ThDP, and 0.5 mM PMSF, and dialyzed against the same buffer at 4 °C overnight. The desalted protein was applied to a Pharmacia Hiload Q Sep (HP) column equilibrated with 20 mM Bis-Tris, 0.5 M EDTA, and 2 mM $MgCl_2$, and the protein was eluted by a linear gradient with 2 M NaCl at a flow rate of 5.0 mL/min. Fractions (4 mL) were collected, and then the procedure in the previous paragraph was followed.

Steady-State Kinetic Analysis was carried out on a CO-BAS-BIO automatic centrifugal analyzer (Roche Diagnostics Corp., Indianapolis, IN) using the NADH/ADH coupled assay. A triple buffer was used (consisting of 50 mM MES, 100 mM Tris, 50 mM acetic acid, 2 mM $MgCl_2$, 1 mM ThDP, and 1 mM EDTA) at the pH values indicated in the figures and tables. This triple buffer system provides a constant ionic strength in the entire pH range used (*19*). Pyruvate, NADH, and ADH were dissolved in Milli-Q water. YPDC was diluted into the pH 6.0 triple buffer to prevent pH-dependent denaturation. The final concentrations of pyruvate in the steady-state kinetic study ranged from 0.05 to 75 mM for the C221D/C222A and C221E/C222A variants and from 0.1 to 60 mM for WT YPDC. NADH concentration was selected to give an initial A_{340} of 1.2−1.4. The ADH concentration was 10−11 units/mL, calculated to be sufficient at all pH values to avoid the coupling enzyme being rate limiting.

The v_o-[S] data were fitted to the Hill equation:

$$v_o/[E_0] = k_{cat}[S]^n/(S_{0.5}^n + [S]^n) \quad (1)$$

$$v_o/[E_0] = k_{cat}[S]^n/\{S_{0.5}^n + [S]^n(1 + [S]/K_i)\} \quad (2)$$

Data that showed no substrate inhibition were analyzed with eq 1; those that did display substrate inhibition were analyzed with eq 2. The Sigma Plot program from SPSS was used for fitting the entire curve, leading to values for k_{cat}, $S_{0.5}$, n_H, and $k_{cat}/S_{0.5}$.

The data for WT YPDC were also fitted to the following equation developed by Alvarez et al. (*12*), assuming two pyruvate-binding sites on each monomer:

$$v_o = V_{max}[S]^2/(A + B[S] + [S]^2) \quad (3)$$

$$v_o = V_{max}[S]^2/\{A + B[S] + [S]^2(1 + [S]/K_i)\} \quad (4)$$

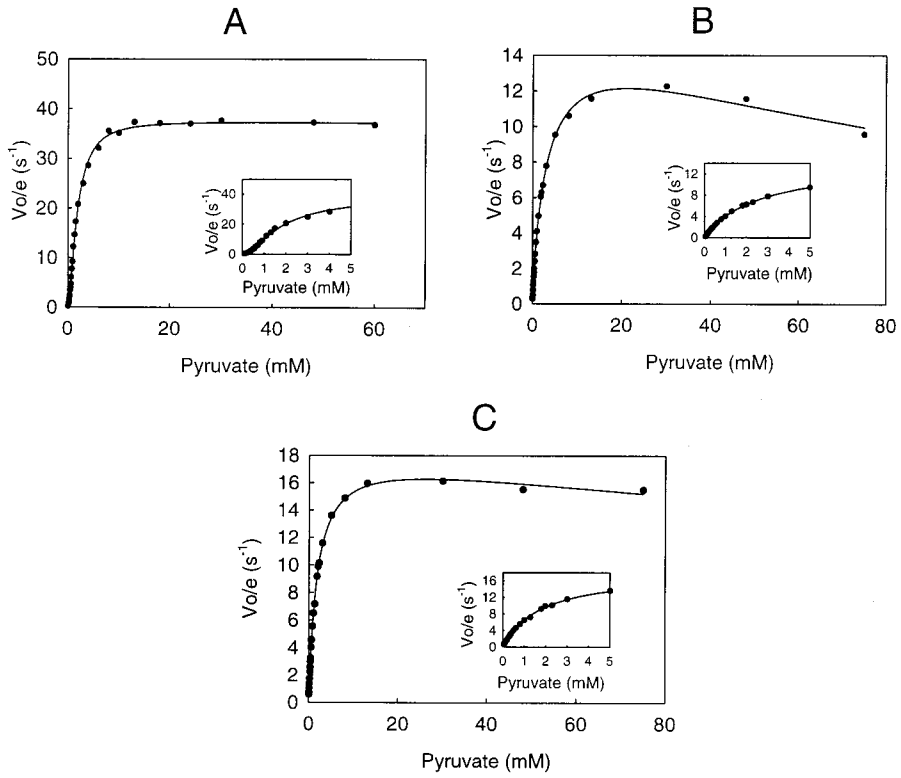

FIGURE 1: v_o vs [S] data for WT-PDC (A), C221D/C222A variant (B), and C221E/C222A variant (C) at pH 6.0. Insets: v_o-[S] at low pyruvate concentration.

The k_{cat}/A and k_{cat}/B values were calculated from fitting the data to these equations. Again, eqs 3 and 4 were used in the absence and presence of substrate inhibition, respectively.

All the apparent pK_a values were determined by fitting the data to eq 5, as an example:

$$V = V_{max}/(1 + 10^{-pKa2}/[H] + [H]/10^{-pKa1}) \qquad (5)$$

Similarly, the apparent pK_a's from the pH dependence of k_{cat}, $k_{cat}/S_{0.5}$, $k_{cat}/S^n_{0.5}$, k_{cat}/A, and k_{cat}/B were determined using the same form as in eq 5, and such pK_a's are listed in Table 6.

Solvent Deuterium Kinetic Isotope Effect Determinations on WT YPDC and Its C221D/C222A, C221E/C222A Variants. 99.9% D_2O was used to make buffers ranging from pD 5.4 to pD 7.5. Pyruvate, NADH, and ADH were also dissolved in D_2O. v_o-[S] data were fitted to the same equations as mentioned under the steady-state kinetic analysis. Parallel analysis in H_2O (pH ranging from 5.0 to 7.5) and in D_2O was carried out with the same enzyme preparation. A particularly useful method to produce reproducible data was to alternate collecting v_o-[S] data first in D_2O, and then in H_2O at the same pL value. A complete steady-state kinetic data set in the entire pL range in both light and heavy water could be produced in 1 day.

RESULTS

Mutagenesis. The alanine residue at position 221 in the C221A/C222A variant was replaced with aspartic acid (D) and glutamic acid (E) via site-directed mutagenesis, yielding substitutions at residues 221 and 222 resulting in the C221D/C222A and C221E/C222A variants. All desired mutations were confirmed by DNA sequencing of the entire gene for each construct. No base changes other than those expected were detected.

Table 1: Steady-State Kinetic Parameters of Wild-Type YPDC and the Variants at pH 6.0[a]

	k_{cat} (s^{-1})	$S_{0.5}$ (mM)	$k_{cat}/S_{0.5}$ ($mM^{-1}\,s^{-1}$)	n_H
WT	37.54 ± 0.32	1.80 ± 0.05	20.81 ± 0.58	1.66 ± 0.05
C221D/C222A	20.57 ± 1.12	2.40 ± 0.29	8.56 ± 1.25	0.98 ± 0.04
C221E/C222A	18.21 ± 0.20	1.47 ± 0.04	12.38 ± 0.36	1.05 ± 0.02

[a] Wild-type YPDC parameters were obtained by fitting the data to eq 1. For the variants, the parameters were calculated by fitting the data to eq 2. All of the errors are standard deviations from the data fitting.

Expression and Purification. Both WT YPDC and the variants were expressed in *E. coli* BL21(DE3) cells. YPDC was found in the cell lysate. After purification, the enzymes exhibited a single band on SDS−PAGE with the protein molecular weight near 60 000, as compared to the theoretical molecular mass of 61 486 Da.

Steady-State Kinetic Analysis. The v_o-[pyruvate] plots at pH 6.0 are presented for WT YPDC and the variants in Figure 1, along with the detailed plot at low pyruvate concentration in the insets. The specific activities of the variants and wild-type YPDC, along with steady-state kinetic parameters, are compared at pH 6.0 and 25 °C in Table 1. The $S_{0.5}$ of the C221D/C222A and C221E/C222A variants at the corresponding pH values is similar to that for the wild-type enzyme. The Hill coefficient of 1.66 for WT YPDC is consistent with positive homotropic cooperativity, i.e., substrate activation. The substrate activation of WT YPDC can also be seen from Figure 1A from the sigmoidicity of the v_o-[S] plot. For the two variants, substrate activation is abolished, as seen in Figure 1B,C from the hyperbolic v_o-[S]

Table 2: Steady-State Kinetic Parameters for Wild-Type YPDC (A) in H_2O[a] and (B) in D_2O[c]

(A) In H_2O[a]

pH	k_{cat} (s^{-1})	$S_{0.5}$ (mM)	n_H	$k_{cat}/S_{0.5}$ ($mM^{-1}\,s^{-1}$)	k_{cat}/A ($mM^{-2}\,s^{-1}$)	k_{cat}/B ($mM^{-1}\,s^{-1}$)	$k_{cat}/S^n_{0.5}$	K^1_i (mM)	K^2_i (mM)
5.0	3.31 ± 0.04	0.96 ± 0.02	1.26 ± 0.03	3.46 ± 0.10	20.84 ± 2.52	4.03 ± 0.22	3.50[b]	185.7 ± 17.39	84.1 ± 12.9
5.4	21.61 ± 0.17	1.66 ± 0.03	1.60 ± 0.03	12.99 ± 0.24	15.51 ± 0.82	24.82 ± 2.52	9.55	413.3 ± 40.56	295.2 ± 32.0
5.7	29.91 ± 0.24	1.53 ± 0.04	1.73 ± 0.06	19.53 ± 0.49	19.74 ± 1.57	52.81 ± 12.51	14.31		2222 ± 2394
6.0	37.54 ± 0.32	1.80 ± 0.05	1.66 ± 0.05	20.81 ± 0.58	22.04 ± 1.85	39.19 ± 6.32	14.13		
6.3	41.79 ± 1.23	2.39 ± 0.14	1.55 ± 0.08	17.48 ± 1.29	18.49 ± 2.30	26.32 ± 4.67	10.87		
6.6	42.44 ± 0.35	3.08 ± 0.07	1.56 ± 0.04	13.80 ± 0.38	10.82 ± 0.85	21.89 ± 2.57	7.32		
6.9	40.58 ± 0.26	4.76 ± 0.08	1.65 ± 0.03	8.52 ± 0.18	3.34 ± 0.13	18.27 ± 1.07	3.11		
7.2	38.11 ± 0.42	7.73 ± 0.18	1.67 ± 0.05	4.93 ± 0.19	1.17 ± 1.14	11.15 ± 1.20	1.26		

(B) In D_2O[c]

pD	k_{cat} (s^{-1})	$S_{0.5}$ (mM)	n_H	$k_{cat}/S_{0.5}$ ($mM^{-1}\,s^{-1}$)	k_{cat}/A ($mM^{-2}\,s^{-1}$)	k_{cat}/B ($mM^{-1}\,s^{-1}$)	$k_{cat}/S^n_{0.5}$	$S^n_{0.5}/K^1_i$ (mM)	K^2_i (mM)
5.7	8.88 ± 0.12	0.97 ± 0.03	1.45 ± 0.05	9.14 ± 0.27	26.76 ± 2.36	14.40 ± 1.28	9.26[b]	194.1 ± 18.9	160.2 ± 12.6
6.0	19.45 ± 0.34	1.00 ± 0.03	1.51 ± 0.06	19.52 ± 0.73	48.34 ± 4.55	33.33 ± 3.94	19.56	149.0 ± 15.9	125.0 ± 10.4
6.3	25.86 ± 0.48	1.21 ± 0.04	1.44 ± 0.05	21.40 ± 0.88	54.62 ± 4.90	31.83 ± 2.92	19.68	153.8 ± 16.3	126.5 ± 9.4
6.6	27.90 ± 0.52	1.27 ± 0.05	1.55 ± 0.06	22.02 ± 0.92	40.40 ± 3.98	39.19 ± 5.74	19.33	247.9 ± 39.1	192.7 ± 24.8
6.9	30.11 ± 0.68	1.67 ± 0.07	1.49 ± 0.06	18.00 ± 0.95	30.87 ± 2.85	27.18 ± 3.13	13.97	224.6 ± 36.4	68.9 ± 18.5
7.2	29.87 ± 0.85	2.11 ± 0.11	1.53 ± 0.07	14.13 ± 0.97	17.82 ± 2.15	22.00 ± 3.78	9.48	323.7 ± 85.0	219.4 ± 41.4
7.5	29.70 ± 1.40	3.17 ± 0.24	1.57 ± 0.08	9.38 ± 1.06	7.73 ± 1.43	13.96 ± 3.80	4.84	144.5 ± 35.4	352.1 ± 189.9

[a] k_{cat}, $S_{0.5}$, n_H, $k_{cat}/S_{0.5}$, and K^1_i were calculated by fitting the data to eq 1 for pH 5.7 to 7.2 and to eq 2 for pH 5.0 to 5.4. k_{cat}/A, k_{cat}/B, and K^2_i were calculated by fitting the data to eq 4 for pH 5.0 to pH 6.6 and to eq 3 for pH 6.9 to 7.2. The errors are standard deviations from data fitting. [b] No error analysis was carried out on this complex function. [c] k_{cat}, $S_{0.5}$, n_H, $k_{cat}/S_{0.5}$, and K^1_i were calculated by fitting the data to eq 2. k_{cat}/A, k_{cat}/B, and K^2_i were calculated by fitting the data to eq 4. The errors are standard deviations of data fitting.

Table 3: Steady-State Kinetic Parameters for the YPDC C221D/C222A Variant (A) in H_2O[a] and (B) in D_2O[b]

(A) In H_2O[a]

pH	k_{cat} (s^{-1})	$S_{0.5}$ (mM)	n_H	$k_{cat}/S_{0.5}$ ($mM^{-1}\,s^{-1}$)	K_i (mM)
5.0	0.85 ± 0.06	0.49 ± 0.09	1.02 ± 0.12	1.72 ± 0.31	40.9 ± 9.0
5.4	3.53 ± 0.07	0.74 ± 0.04	1.05 ± 0.03	4.77 ± 0.25	151.9 ± 18.1
5.7	9.55 ± 0.13	1.56 ± 0.05	1.00 ± 0.02	6.12 ± 0.23	163.1 ± 12.0
6.0	20.57 ± 1.12	2.40 ± 0.29	0.98 ± 0.04	8.56 ± 1.25	134.1 ± 39.0
6.3	21.49 ± 0.32	2.80 ± 0.10	1.03 ± 0.02	7.68 ± 0.33	303.6 ± 27.1
6.6	25.21 ± 0.19	4.22 ± 0.07	1.04 ± 6.9 × 10^{-3}	5.98 ± 0.14	352.3 ± 16.5
6.9	27.57 ± 1.37	9.34 ± 0.94	0.98 ± 0.03	2.95 ± 0.54	158.8 ± 23.7
7.2	21.16 ± 1.07	13.53 ± 1.33	0.97 ± 0.02	1.56 ± 0.33	172.4 ± 26.0
7.5	12.84 ± 2.28	22.24 ± 6.91	0.97 ± 0.05	0.58 ± 0.52	81.9 ± 27.6

(B) In D_2O[b]

pD	k_{cat} (s^{-1})	$S_{0.5}$ (mM)	n_H	$k_{cat}/S_{0.5}$ ($mM^{-1}\,s^{-1}$)	K_i (mM)
5.4	0.429 ± 0.01	0.22 ± 0.02	1.22 ± 0.11	1.92 ± 0.14	
5.7	1.50 ± 0.06	0.40 ± 0.04	0.92 ± 0.06	3.77 ± 0.40	124.9 ± 25.2
6.0	4.26 ± 0.12	0.84 ± 0.07	0.89 ± 0.03	5.07 ± 0.41	101.8 ± 11.7
6.3	8.69 ± 0.68	0.89 ± 0.17	1.05 ± 0.12	9.79 ± 2.00	314.1 ± 245.3
6.6	13.91 ± 0.10	1.34 ± 0.02	1.09 ± 0.01	10.40 ± 0.20	728.5 ± 76.7
6.9	19.31 ± 0.24	2.16 ± 0.06	1.02 ± 0.01	8.96 ± 0.31	229.5 ± 14.5
7.2	19.13 ± 0.5	2.57 ± 0.18	1.03 ± 0.03	7.45 ± 0.62	287.8 ± 49.5
7.5	19.08 ± 0.52	3.69 ± 0.21	1.12 ± 0.03	5.18 ± 0.40	329.1 ± 70.2

[a] All of the parameters were calculated by fitting the data to eq 2, and all of the errors are standard deviations from data fitting. [b] All of the parameters were calculated by fitting the data to eq 2, and all of the errors are standard deviations from data fitting.

curves. The elimination of substrate activation is also confirmed with the calculated Hill coefficients of 0.98 and 1.02 for C221D/C222A and C221E/C222A variants, respectively. The k_{cat}'s of the YPDC C221D/C222A and C221E/C222A variants are only modestly reduced by substitution at position C221, less than 2-fold at pH 6.0, and by approximately 30% at the optimal pH values.

pL-Dependence of Steady-State Kinetic Parameters and Solvent Deuterium Isotope Kinetic Effects (SKIE). The steady-state kinetic parameter-pH (pD) profiles of WT YPDC and C221D/C222A, C221E/C222A variants in protiated (and deuterated) water are shown in Figures S1A, S1B, S2A, S2B, S3A, and S3B, respectively, of Supporting Information. Summaries of the parameters at different pH(D) of both WT YPDC and the variants are listed in Tables 2, 3, and 4. The $^Dk_{cat}/K_m$ (and related) and $^Dk_{cat}$ values are summarized in Table 5. The pK_a's deduced from the pH(pD)-dependent kinetic parameters are given in Table 6.

The value of $^Dk_{cat}$ for wild-type YPDC and both variants is "normal" (i.e., greater than unity). The values of $^Dk_{cat}/S^n_{0.5}$, or $^Dk_{cat}/A$ for wild-type YPDC and of $^Dk_{cat}/S_{0.5}$ (or $^Dk_{cat}/K_m$, since the Hill coefficient is unity) of both variants are "inverse", i.e., less than unity. Finally, the values of $^Dk_{cat}/S_{0.5}$ and $^Dk_{cat}/B$ of wild-type YPDC are nearly unity. All SKIE

Table 4: Steady-State Kinetic Parameters for the YPDC C221E/C222A Variant (A) in H_2O[a] and (B) in D_2O[a]

(A) In H_2O[a]

pH	k_{cat} (s^{-1})	$S_{0.5}$ (mM)	n_H	$k_{cat}/S_{0.5}$ ($mM^{-1}\,s^{-1}$)	K_i (mM)
5.0	0.80 ± 0.02	0.34 ± 0.02	1.00 ± 0.06	2.35 ± 0.17	99.8 ± 10.9
5.4	3.21 ± 0.07	0.62 ± 0.04	1.00 ± 0.04	5.18 ± 0.33	128.0 ± 12.8
5.7	8.43 ± 0.16	0.86 ± 0.04	1.10 ± 0.03	9.76 ± 0.48	643.8 ± 167.6
6.0	18.21 ± 0.20	1.47 ± 0.04	1.05 ± 0.02	12.38 ± 0.36	339.3 ± 27.3
6.3	24.32 ± 0.28	2.14 ± 0.06	1.03 ± 0.01	11.37 ± 0.37	436.1 ± 42.9
6.6	29.53 ± 0.47	3.25 ± 0.12	1.00 ± 0.02	9.09 ± 0.42	454.5 ± 56.5
6.9	31.93 ± 0.75	4.52 ± 0.24	1.00 ± 0.02	7.07 ± 0.51	360.8 ± 51.5
7.2	30.10 ± 0.77	7.92 ± 0.42	1.00 ± 0.02	3.80 ± 0.34	357.6 ± 49.6
7.5	23.00 ± 1.16	13.90 ± 1.31	1.00 ± 0.02	1.65 ± 0.35	131.2 ± 16.8

(B) In D_2O[a]

pD	k_{cat} (s^{-1})	$S_{0.5}$ (mM)	n_H	$k_{cat}/S_{0.5}$ ($mM^{-1}\,s^{-1}$)	K_i (mM)
5.4	0.45 ± 0.06	0.21 ± 0.07	1.00 ± 0.34	2.15 ± 0.76	68.7 ± 35.6
5.7	2.17 ± 0.10	0.39 ± 0.05	1.00 ± 0.10	5.49 ± 0.70	75.0 ± 12.8
6.0	6.50 ± 0.10	0.66 ± 0.03	1.02 ± 0.03	9.92 ± 0.42	111.2 ± 7.0
6.3	13.17 ± 0.18	0.97 ± 0.03	1.01 ± 0.02	13.58 ± 0.52	198.6 ± 14.6
6.6	20.42 ± 0.50	1.44 ± 0.09	1.00 ± 0.03	14.21 ± 0.96	170.7 ± 18.5
6.9	21.92 ± 0.34	1.45 ± 0.05	1.06 ± 0.02	15.15 ± 0.64	398.8 ± 53.2
7.2	24.81 ± 0.72	2.24 ± 0.16	1.00 ± 0.03	11.07 ± 0.91	185.7 ± 23.4
7.5	23.44 ± 0.71	2.71 ± 0.18	1.08 ± 0.03	8.66 ± 0.73	360.9 ± 75.7

[a] All of the parameters were calculated by fitting the data to eq 2 and all of the errors are standard deviations from data fitting.

Table 5: SKIE Parameters for Wild-Type YPDC and the C221D(E)/C222A Variants[a]

	$^Dk_{cat}$	$^Dk_{cat}/S_{0.5}$	$^Dk_{cat}/S^n_{0.5}$	$^Dk_{cat}/A$	$^Dk_{cat}/B$
WT	1.30 ± 0.01	0.92 ± 0.01	0.76 ± 0.02	0.48 ± 0.03	1.06 ± 0.01
C221D/C222A	1.45 ± 0.04	0.82 ± 0.05			
C221E/C222A	1.26 ± 0.03	0.80 ± 0.01			

[a] $^Dk_{cat}$, $^Dk_{cat}/S_{0.5}$, $^Dk_{cat}/S^n_{0.5}$, $^Dk_{cat}/A$, $^Dk_{cat}/B$ were calculated from the ratio of the maximal values of the parameters by inspecting the parameter-pH(D) profile. The error is the average error of two sets of identical experiments.

Table 6: Apparent $_pK_a$ Values for Wild-Type YPDC and Its C221D/C222A and C221E/C222A Variants[a]

		k_{cat}		pH independent	$k_{cat}/S_{0.5}$		pH independent
		p*K*a1	p*K*a2	k_{cat} (s^{-1})	p*K*1	p*K*a2	$k_{cat}/S_{0.5}$ ($mM^{-1}\,s^{-1}$)
WT	(H_2O)	5.63 ± 0.13	7.59 ± 0.24	52.80 ± 5.52	5.86 ± 0.21	6.19 ± 0.20	50.17 ± 15.47
	(D_2O)	6.00 ± 0.12	8.17 ± 0.34	36.21 ± 3.58	6.05 ± 0.19	6.97 ± 0.18	38.21 ± 8.24
C221D/C222A	(H_2O)	6.25 ± 0.18	7.14 ± 0.20	46.78 ± 10.33	6.04 ± 0.19	6.13 ± 0.19	27.27 ± 8.98
	(D_2O)	6.84 ± 0.16	7.58 ± 0.23	38.09 ± 8.72	6.36 ± 0.17	6.99 ± 0.18	20.43 ± 4.76
C221E/C222A	(H_2O)	6.33 ± 0.10	7.45 ± 0.13	50.40 ± 5.79	5.99 ± 0.16	6.36 ± 0.16	28.54 ± 6.87
	(D_2O)	6.63 ± 0.17	7.75 ± 0.30	38.99 ± 8.23	6.22 ± 0.12	7.18 ± 0.13	25.36 ± 3.65

		k_{cat}/A		k_{cat}/B		$k_{cat}/S^n_{0.5}$	
		p*K*a1	p*K*a2	p*K*a1	p*K*a2	p*K*a1	p*K*a2
WT	(H_2O)	4.52 ± 0.68	6.48 ± 0.31	5.13 ± 2.62	6.65 ± 2.65	5.52 ± 0.32	6.28 ± 0.33
	(D_2O)	6.09 ± 0.33	6.49 ± 0.35	6.13 ± 0.30	6.86 ± 0.28	6.21 ± 0.27	6.53 ± 0.25
C221D/C222A	(H_2O)						
	(D_2O)						
C221E/C222A	(H_2O)						
	(D_2O)						

[a] All pK_a values were calculated from eq 5. The errors are standard deviations from the data fitting. The "pH-independent" parameters are those given by the computer fit to eq 5.

parameters were calculated from the ratio of the maximal values of the parameter-pH(D) profile. The SKIE parameters for the two variants represent the average of two sets of data obtained in identical experiments; the SKIE for WT YPDC was carried out on two different enzyme preparations. To demonstrate the SKIE trends with increasing substrate concentration for the wild-type YPDC, the v_o-pL plots were superimposed for increasing (but single) substrate concentrations in Figure 2. It is clearly seen that the SKIE changes from inverse at low, to near 1.0 for substrate concentration near $S_{0.5}$, to normal at higher substrate concentrations. As seen in Figure 2, whether the SKIE is inverse or normal for a particular substrate concentration range, is in little doubt, as is the trend of the SKIE with increasing substrate concentration. These plots affirm that the deduced SKIEs for the wild-type YPDC are on solid ground. This was important to demonstrate, since there appears to be discrepancy with earlier data only at intermediate substrate concentrations, with $^Dk_{cat}$/B inverse with a value of 0.5−0.6 in the earlier study (*12*), as compared to near unity in our study.

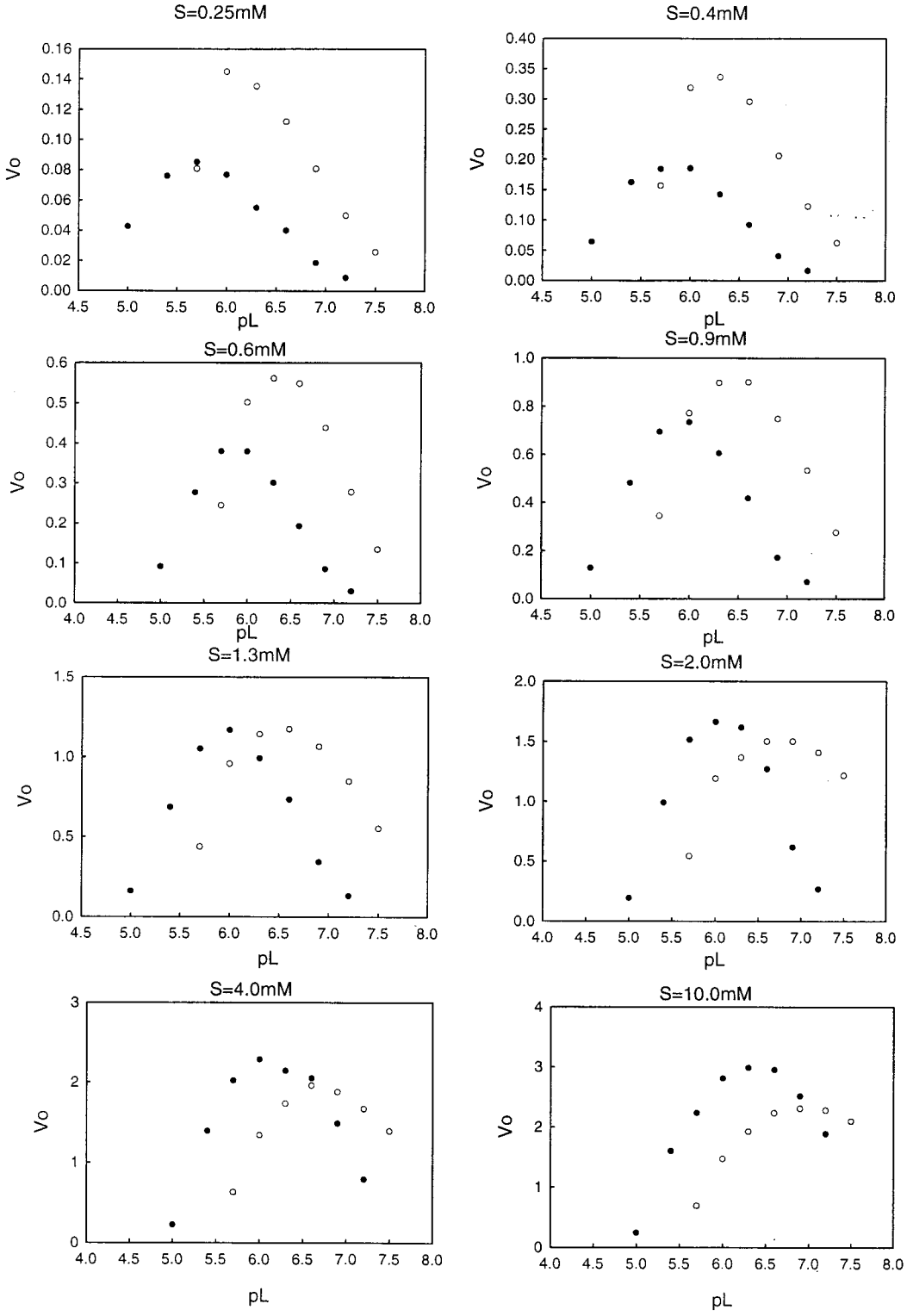

FIGURE 2: Plot of v_o-pL for the pyruvate concentrations indicated above each plot. Open circles in heavy water, closed circles in light water.

Effects of Pyruvamide on the Kinetic Constants of the Variants. The v_o-[pyruvate] plots were determined for the C221D/C222A variant at pH 6.0 in the absence and presence of 80 mM pyruvamide (preincubation with pyruvamide for 5 min), a substrate surrogate capable of activating the wild-type YPDC, and yielded the following results (first number in the absence, second in the presence of pyruvamide; no units are listed for simplicity): V_{max}, 1.23 ± 0.069 and 1.16 ± 0.069; K_m, 1.79 ± 0.041 and 2.57 ± 0.34; n (Hill coefficient), 1.036 ± 0.012 and 1.000 ± 0.054; and K_i, 316 ± 27 and 146 ± 30. We conclude that pyruvamide has virtually no effect on V_{max}, causes a small increase of K_m, and reduces the K_i, i.e., it is an inhibitor even at this concentration, well below the 300 mM concentration used for determination of the YPDC structure in the presence of pyruvamide (*15*).

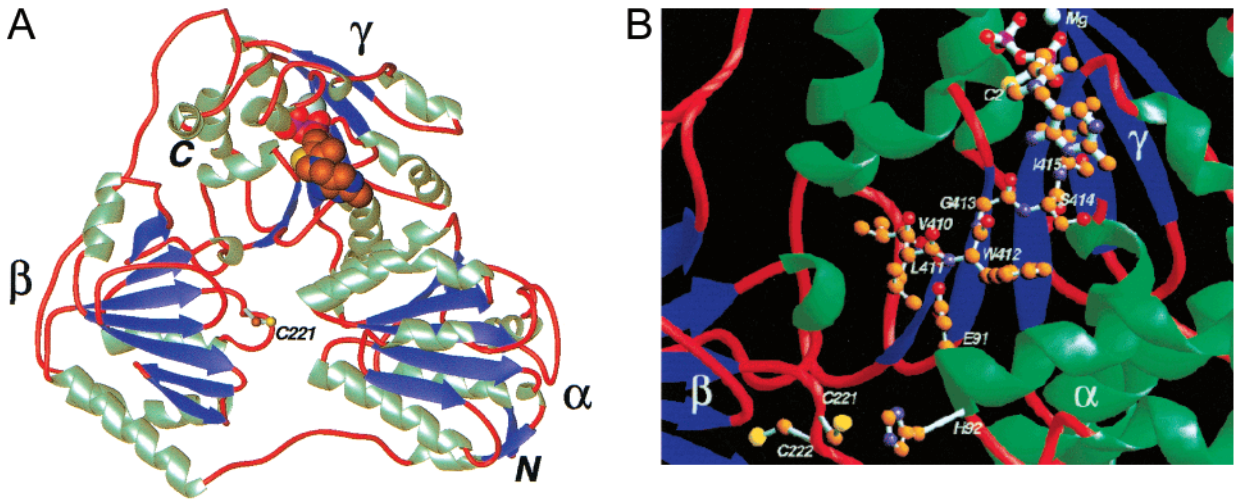

FIGURE 3: Location of C221 with respect to the regulatory signal transduction pathway to ThDP on yeast pyruvate decarboxylase. (A) A single YPDC subunit is shown; the protein is represented as a ribbon drawing, whereas the ThDP cofactor is represented as a space filling model. (B) The substrate activation pathway from C221 to ThDP.

Scheme 1

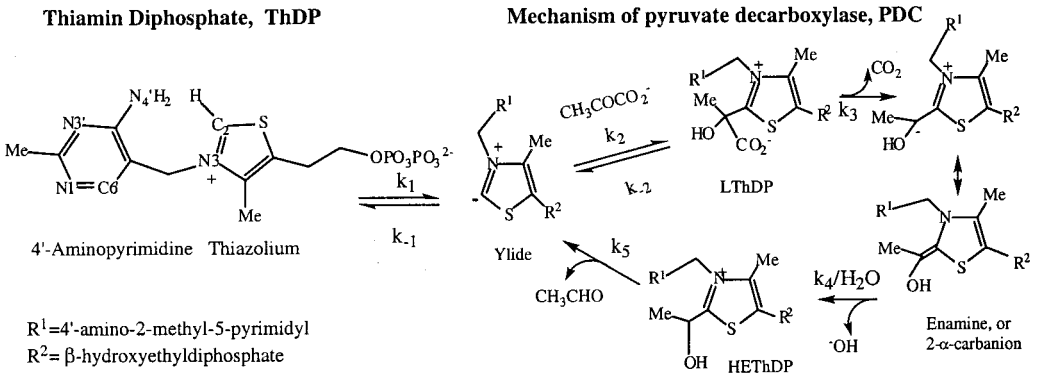

DISCUSSION

As seen in Figure 3, the residue C221 is located not only >20 Å from the active center with the ThDP cofactor, whose C2 and N4′ atoms (Scheme 1) constitute the key catalytic atoms for the reaction, but C221 is also on a different domain than the cofactor. The information originating from the pyruvate bound at C221 must traverse a pathway over all three domains of the same subunit to reach the active center. It is all the more impressive then that even very subtle changes in substitution at this position have such dramatic effects on the activation, while having only more modest effects on the k_{cat} of the enzyme.

Steady-State Kinetic Results. (a) Effects on Specific Activity and k_{cat}. Depending on the preparation, the optimal specific activities are 5−10 units/mg for the C221S, 10−15 for the Ala, and 20−28 units for Asp and Glu substituents, as compared to 40−60 units/mg for the wild-type YPDC. The pH effects appear to be very similar on k_{cat} for the variants and the wild-type enzyme, suggesting that the rate-limiting steps under conditions of saturating pyruvate concentration are under the influence of the same groups, irrespective of the substitutions at residue 221. Furthermore, the results support once more the notion that substitutions at C221 have only modest effects on the kinetic barriers starting with the decarboxylation step in Scheme 1. Elsewhere, data have been presented on variants resulting from substitutions of the active center acid−base residues D28, H114, H115, E477 (*20*), and E51 (*17*). All five of these residues have significant effects on k_{cat}; at least 100 times larger reductions result from their substitutions than with the C221 variants.

(b) Effects on the Hill Coefficient. The Hill coefficients for the C221 substituents are <1.0 for Ser (0.8−0.9), essentially 1.0 within experimental error for the Ala, Glu, and Asp substituents, as compared to 1.6−2.0 (again depending on buffer, preparation) for the wild-type YPDC. These numbers are of significance for several reasons: (i) The most important conclusion is that YPDC with no activation is still active. (ii) The explanation for a number <1.0 suggests complications not yet discussed for YPDC. In a different paper, we suggested that the number is consistent with a mechanism in which a functional dimer with more than two substrate-binding sites, rather than a monomer with two substrate-binding sites, is the minimal catalytic unit (*16*). The important finding with the new variants here presented is that the magnitude of the Hill coefficient is unity (within experimental error) in the entire pH range.

The finding that the Hill coefficient is unity could have multiple origins, either a fully unactivated enzyme form (or a form that cannot be activated), or a fully activated enzyme form. We had earlier shown that the C221S and C221A substitutions convert the enzyme into a form that can no

longer be activated. With wild-type YPDC, the addition of pyruvamide has the latter effect, i.e., preincubation with pyruvamide leads to hyperbolic v_o-[S] plots, and it is converted to the activated form.

It is of particular importance that while the Hill coefficient remains near 1.0 for all C221 substitutions, the k_{cat} increases from Ser to Ala to Asp (and Glu), with the K_m decreasing successively. In fact, the $S_{0.5}$ is nearly the same for the wild-type YPDC and the C221D/C222A and C221E/C222A variants, and these variants achieve nearly 70% of the k_{cat} of the wild-type enzyme at their optimum pH.

(c) Effects on k_{cat}/K_m and their pH Dependencies. As expected from the Hill coefficient, the data for the wild-type YPDC and the C221D/C222A and C221E/C222A variants differed mostly in events starting with binding of substrate and culminating in decarboxylation. In the previous analysis of wild-type YPDC kinetics presented by the groups of Schellenberger and Hübner at Halle and Schowen in Kansas (referred to as the SHS model), the steady-state kinetic data were partitioned into three regimes of substrate concentration, saturating (substrate independent, k_{cat}), midrange (first order in substrate, k_{cat}/B), and low concentration (approaching zero, second order in substrate to account for the sigmoidal v_o-[S] plots, k_{cat}/A). According to this formulation, k_{cat}/A accounts for transition states starting from binding of the first substrate, presumably at C221, and culminating with decarboxylation, while k_{cat}/B includes transition states starting with substrate binding to the *substrate-activated* enzyme and culminating with decarboxylation.

In practical terms, while isolation of the low and high substrate terms is feasible, in our hands, the B term is subject to greater uncertainty, a problem accentuated in the pH-dependent kinetic studies. Pragmatically, the Hill coefficient provides less specific assignment of the rate parameters, but the $S_{0.5}$ and/or $S^n_{0.5}$, and (the derived $k_{cat}/S_{0.5}$ or $k_{cat}/S^n_{0.5}$ parameters) provide solid but "averaged" values for the binding, typically leading to pH profiles that are highly reproducible and consistent. We have also shown elsewhere (*16*) that under certain conditions the SHS parameters and Hill parameters are nearly the same: the closest Hill analogue of k_{cat}/A is $k_{cat}/S^n_{0.5}$, while the Hill analogue of k_{cat}/B is $k_{cat}/S_{0.5}$. We therefore show all of these plots so that the reader can obtain a better appreciation of the experimental obstacles (see Supporting Information).

The steady-state kinetics of wild-type YPDC in the entire pH-range of activity (as low as 4.6, as high as 7.8) have been studied extensively by several people at Rutgers over the past decade. While the shape of the k_{cat}-pH profile is indeed similar to that reported for the SHS model (see Supporting Information for ref *12*), for wild type and several YPDC variants, invariably *bell-shaped curves result for plots of k_{cat}/K_m vs pH (and similar plots for other related parameters).* This has been shown not only for wild-type enzyme, but for variants at residues C221, H92, E91, and W412 on the putative regulatory pathway, as well as on the active center variants at residues D28, H114, H115, E51, I415, and E477.

In this report, the entire pH dependence of the v_o-[S] plots is described both in light and heavy water. As seen in Table 6 and in Supporting Information, there is a shift to more alkaline values on transfer from light to heavy water, as anticipated. The number of data points is insufficient to enable us to draw any conclusions regarding the apparent pK_a values, other than the shape of the k_{cat}/K_m-type profiles described in the previous paragraph. Interestingly, there appears to be one pK_a shift that is very likely outside of experimental error: the pK_a on the acidic limb of the k_{cat}-pH profiles experiences a shift to more alkaline values on substitution of C221 to aspartate or glutamate, further affirming that there is signal transduced from the regulatory to the catalytic center.

Solvent Kinetic Isotope Effects. (a) Effects on k_{cat}. As published for YPDC (*12*), ZmPDC (*13*), BFD (*14*), and most recently for the C221A/C222A variants (*8*), the $^Dk_{cat}$ (or ^DV) is normal (>1.0) for all of these related enzymes. Most relevant to this paper, the $^Dk_{cat}$ is >1 again for the C221D/C222A and C221E/C222A variants, as well as for the wild-type enzyme redetermined in this laboratory. This is strong evidence that (a) In the rate-determining step of the post-decarboxylation regime of the overall reaction hydrogen bonding is stronger in the transition state; and (b) The perturbations at the regulatory site do not significantly influence the rate-limiting step in the post-decarboxylation regime of the reaction.

(b) Effects on k_{cat}/K_m and Related Terms. Hypothetically, results with Hill coefficients of unity could imply the presence of enzyme forms, or conformations, with no activation (enzyme forms that cannot be activated), or full activation. Therefore, the SKIEs obtained for the C221 variants here presented may correspond to any of these forms, or to anything between, e.g., frozen into an intermediate state. With a Hill coefficient near 1.0, the $S_{0.5}$ and K_m values are interchangeable.

The $^Dk_{cat}/S_{0.5}$ SKIE observed with the C221A/C222A variant was 0.62 ± 0.02, with the C221D/C222A it is 0.82 ± 0.05, and with the C221E/C222A variant it is 0.80 ± 0.01. Interestingly, the SKIE becomes less inverse as the activity of the variant increases. Possibly, installation of the negative charge mimics the charge, and its interaction with its surroundings, of a pyruvate molecule covalently bound to C221 as a thiohemiketal adduct.

To what value on wild-type enzymes shall we compare our results with these variants? The values from our studies for the wild-type YPDC are $^Dk_{cat}/A = 0.48$, $^DV/S^n_{0.5} = 0.76$, $^Dk_{cat}/B = 1.06$, and $^Dk_{cat}/S_{0.5} = 0.92$, as compared with $^Dk_{cat}/K_m = 1.25$ for ZmPDC and $^Dk_{cat}/K_m = 1.5$ for BFD (a ThDP enzyme with a phenyl group in place of the methyl group of pyruvate in the substrate). Neither ZmPDC nor BFD is subject to substrate activation; hence, it is reasonable to assume that ZmPDC and BFD represent fully activated enzymes. Our newly determined values for the wild-type YPDC of $^Dk_{cat}/B = 1.06$, and $^Dk_{cat}/S_{0.5} = 0.92$ are in better agreement with the $^Dk_{cat}/K_m = 1.25$ for ZmPDC, again consistent with the notion that the $^Dk_{cat}/B$ and $^Dk_{cat}/S_{0.5}$ values on the wild-type enzyme reflect on the behavior of substrate-activated enzyme species.

At the same time, a comparison of the $^Dk_{cat}/K_m$ for the C221A/C222A (0.62), C221D (or E)/C222A (0.82, 0.80) variants to the values of $^Dk_{cat}/A = 0.48$ ($^DV/S^n_{0.5} = 0.76$) and $^Dk_{cat}/B = 1.06$ ($^Dk_{cat}/S_{0.5} = 0.92$) observed with the wild type YPDC, respectively, is useful. It is plausible to conclude that installation of the negatively charged residue at position 221

"freezes" the conformational equilibrium of the YPDC, selecting a conformation somewhere between fully activated wild-type enzyme and enzyme that cannot be activated. Let us suppose that the C221A/C222A variant is an example of the unactivated form, in which the hydrogen bonds are stronger in the free enzyme than in the rate-limiting transition state. In the substrate-activated YPDC, the hydrogen bonds are nearly the same strength as those in the rate-limiting transition state. With the C221D(E)/C222A variants, there is relatively little change in hydrogen bonding as well in going through the rate-limiting transition state, although the direction of change is still the same as with the C221A/C222A variant.

The results here reported for the wild-type enzyme require modification of the conclusions reached in the earlier study (*12*), which reported an inverse SKIE for both the $^{D}k_{cat}/A$ term and the $^{D}k_{cat}/B$ term. Our numbers simply are not consistent with an inverse $^{D}k_{cat}/B$ of 0.5. The small temperature differences (25 °C in this study, 30 °C in the earlier one), differences in buffer (the triple buffer in this study and citric acid in the earlier one), or even enzyme preparations (we used the His_6-tagged recombinant YPDC from *E. coli*, the earlier one used YPDC isolated from yeast) are unlikely to account for the differences, especially since the $^{D}k_{cat}$ and $^{D}k_{cat}/A$ terms are rather similar in the two studies.

Our new values for the $^{D}k_{cat}/B$ term of the wild-type YPDC, along with our results on the C221A/C222A, C221D/C222A, and C221E/C222A variants lead us to the following interpretation, consistent with all of the SKIE data: (i) The earlier hypothesis that the -SH group of C221 is responsible for the observed inverse SKIE on $^{D}k_{cat}/A$ is virtually ruled out by the results on the C221-substituted variants. Some years ago, we had already reported that the thiolate ionization state of C221 at pH 6.0 deduced from two independent experimental measurements was inconsistent with that hypothesis (*3*). (ii) Enzyme forms of YPDC with no apparent activation according to the Hill criterion can still be quite active, with the C221D/C222A and C221E/C222A variants approaching the activity of fully substrate-activated enzyme. (iii) The results on the C221A/C222A variant suggest that this is a good model for the unactivated form of the enzyme, with the value of $^{D}k_{cat}/K_m$ being reminiscent of the value of $^{D}k_{cat}/A$ observed with the wild-type enzyme. At the same time, the SKIE on $^{D}k_{cat}/K_m$ for the C221D/C222A and C221E/C222A variants approaches the value of $^{D}k_{cat}/B$ found for the wild-type enzyme, suggesting that these variants are a model for the substrate-activated YPDC. (iv) The results also tend to negate the recent suggestion, based on the location of pyruvamide on YPDC [one at the active center, the second between the β and γ domains, bonded in a fashion inappropriate for pyruvate binding (*15*)] that C221 is not the location of substrate activation. In fact, the results of that study suggested that at the high pyruvamide concentrations utilized, pyruvamide can be found at the catalytic center, hence inhibit the enzyme. Our results with pyruvamide and the C221D/C222A variant clearly confirm such an inhibitory role. (v) It appears that substrate activation increases the SKIE from the strongly inverse value to almost no SKIE, suggesting that hydrogen bonding become weaker in the substrate-activated state than in the unactivated free enzyme.

Finally, since our results have virtually ruled out C221SH interacting with pyruvate as the source of the observed inverse SKIE on $^{D}k_{cat}/A$, what is the locus of the hydrogen bonding changes/proton transfer(s) that give rise to this strong inverse SKIE? We believe that the results summarized above, supported by the data on the C221-substituted enzymes, are fully consistent with all of the SKIE observations being pertinent to transition state structural changes at the active center, rather than at the regulatory site, but that the signal is indeed transduced from C221 to ThDP. There is more evidence accumulating, supported by the recent report on the C221A/C222A variant, that ionization of the key thiazolium C2H could become rate limiting in the unactivated enzyme form. The inverse SKIE suggests that the fractionation factor in the ground state be less than unity. Of course, SH ionization is one possible source of this. In general, a "low-barrier hydrogen bond" would give rise to such fractionation factors. In a totally different system, involving serine protease active centers both in their native state and bound to tight-binding peptide boronic acid "transition-state analogues", we found that the hydrogen bond between the histidine $N^{\delta 1}$ of the active site catalytic triad and the aspartate, but not the hydrogen bond from the histidine $N^{\epsilon 2}$ site, has a low fractionation factor (*21*). We suggest that the low fractionation factor required to give rise to the inverse SKIE at low substrate concentrations for the wild-type and the C221A/C222A variant is a property of the C2H to N4′-imino nitrogen interaction on ThDP itself. Indeed, there are some data in the literature indicating that CH bonds at trigonal and digonal carbon centers are characterized by fractionation factors less than unity (*22*). Concomitant with this event, there could also be loosening of the three highly conserved hydrogen bonds around the 4′-aminopyrimidine ring, also contributing to the inverse SKIE. In other words, the inverse SKIE at low substrate concentrations clearly signals tighter binding in the ground state than in the rate-limiting transition state. At the same time, substrate activation increases the rate of C2H exchange, and a step different from C2H to N4′-imino proton-transfer becomes rate-limiting, a step in which there is little if any hydrogen bonding changes in the transition state. In the post-decarboxylation regime, there is a normal SKIE for all of the related ThDP enzymes, where there are possible proton transfers at a number of reaction steps.

ACKNOWLEDGMENT

The authors are grateful to Professor Richard Schowen of the University of Kansas for helpful advice with the protocol for SKIE experiments, to Professor Phil Huskey, and to Dr. Eduard Sergienko of this department for discussions of the results.

SUPPORTING INFORMATION AVAILABLE

Six figures (S1A, S1B, S2A, S2B, S3A, S3B) with plots of pH-dependent steady-state kinetic constants listed in Tables 2−4. This information is available free of charge via the Internet at http://pubs.acs.org.

REFERENCES

1. Zeng, X., Farrenkopf, B., Hohmann, S., Dyda, F., Furey, W., and Jordan, F. (1993) *Biochemistry 32*, 2704−2709.
2. Baburina, I., Gao, Y., Hu, Z., Jordan, F., Hohmann, S., and Furey, W. (1994) *Biochemistry 33*, 5630−5635.

3. Baburina, I., Moore, D. J., Volkov, A., Kahyaoglu, A., Jordan, F., and Mendselsohn, R. (1996) *Biochemistry 35*, 10249−10255.
4. Baburina, I., Li, H., Bennion, B., Furey, W., and Jordan, F. (1998) *Biochemistry 37*, 1235−1244.
5. Baburina, I., Dikdan, G., Guo, F., Tous, G. I., Root, B., and Jordan, F. (1998) *Biochemistry 37*, 1245−1255.
6. Li, H., Furey, W., Jordan, F. (1999) *Biochemistry*, *38*, 9992−10003.
7. Li, H., Jordan, F. (1999) *Biochemistry 38*, 10004−10012.
8. Wang, J., Golbik, R., Seliger, B., Spinka, M., Tittmann, K., Hübner, G., and Jordan, F. (2001) *Biochemistry 40*, 1755−1763.
9. Hübner, G., König, S., and Schellenberger, A. (1988) *Biomed. Biochim. Acta 47*, 9−18.
10. Dyda, F., Furey, W., Swaminathan, S., Sax, M., Farrenkopf, B., and Jordan, F. (1993) *Biochemistry 32*, 6165−6170.
11. Arjunan, D., Umland, T., Dyda, F., Swaminathan, S., Furey, W., Sax, M., Farrenkopf, B., Gao, Y., Zhang, D., and Jordan, F. (1996) *J. Mol. Biol. 256*, 590−600.
12. Alvarez, F. J., Ermer, J., Hübner, G., Schellenberger, A., and Schowen, R. L. (1995) *J. Am. Chem. Soc. 117*, 1678−1683.
13. Sun, S., Duggleby, R. G., and Schowen, R. L. (1995) *J. Am. Chem. Soc. 117*, 7317−7322.
14. Weiss, P. M., Garcia, G. A., Kenyon, G. L., Cleland, W. W., and Cook, P. F. (1988) *Biochemistry 27*, 2197−2205.
15. Lu, G., Dobritzsch, D., Baumann, S., Schneider, G., and König, S. (2000) *Eur. J. Biochem. 267*, 861−868.
16. Sergienko, E. A., and Jordan, F. (2001) *Biochemistry 40*, 7382−7403.
17. Gao, Y. (2000) Ph.D. Dissertation, Rutgers University Graduate Faculty at Newark.
18. Wang, J. (2001) Ph.D. Dissertation, Rutgers University Graduate Faculty at Newark.
19. Ellis, K. J., and Morrison, J. F. (1982) *Methods Enzymol. 87*, 405−427.
20. Liu, M., Sergienko, E., Guo, F., Wang, J., Tittmann, K., Hübner, G., Furey, W., and Jordan, F. (2001) *Biochemistry 40*, 7355−7368.
21. Bao, D., Huskey, W. P., Kettner, C. A., and Jordan, F. (1999) *J. Am. Chem. Soc. 121*, 4684−4689.
22. Cleland, W. W. (1982) *Methods Enzymol. 64B*, 104−125.

BI0112964